

MobiVSR: A Visual Speech Recognition Solution for Mobile Devices

Nilay Shrivastava*
NSIT-Delhi
nilays.co@nsit.net.in

Astitwa Saxena*
NSIT-Delhi
astitwas.co@nsit.net.in

Yaman Kumar*
Adobe Systems, Noida
ykumar@adobe.com

Rajiv Ratn Shah
IIIT-Delhi
rajivrtn@iiitd.ac.in

Debanjan Mahata
Bloomberg LP
dmahata@bloomberg.net

Amanda Stent
Bloomberg LP
astent@bloomberg.net

Abstract

Visual speech recognition (VSR) is the task of recognizing spoken language from video input only, without any audio. VSR has many applications as an assistive technology, especially if it could be deployed in mobile devices and embedded systems. The need for intensive computational resources and large memory footprint are two of the major obstacles in developing neural network models for VSR in a resource constrained environment. We propose a novel end-to-end deep neural network architecture for word level VSR called MobiVSR with a design parameter that aids in balancing the model’s accuracy and parameter count. We use depthwise-separable 3D convolution for the first time in the domain of VSR and show how it makes our model efficient. MobiVSR achieves an accuracy of 73% on a challenging Lip Reading in the Wild dataset with 6 times fewer parameters and 20 times lesser memory footprint than the current state of the art. MobiVSR can also be compressed to 6 MB by applying post training quantization.

1 Introduction

Visual speech recognition (VSR) is the task of recognizing spoken language from video input only, without any audio. Similar to ASR (audio speech recognition), VSR has a multitude of applications. In general, VSR can be used to augment/replace audio speech recognition for situations where speech cannot be heard or produced. For example, if a person has a laryngectomy or voice-box cancer, dysarthria or in a situation where one needs to understand a speaker in a noisy environment. The specific aim of this work is to make VSR technology deployable, especially in mobile environments (such as cars) and on hand-held devices (as an assistive technology).

However the broader aim of this work is to provide a new deep learning construct to optimize deep learning frameworks for video classification tasks. We show this by taking lipreading as a language recognition problem on top of a video classification task.

Recent research in VSR has focused primarily on either recognizing language (Chung and Zisserman, 2016a; Chung et al., 2017), or reconstructing it (Kumar et al., 2018b,a). The application of deep learning techniques has produced models that perform substantially better on lip reading datasets than earlier methods (Petridis et al., 2017; He et al., 2016). However, the major challenge for all these models is to overcome the unique challenges presented at the time of actual use or deployment.

For example, the state-of-the-art model for word level VSR (Stafylakis and Tzimiropoulos, 2017) uses a novel architecture that incorporates a 3D convolution kernel as a front-end to extract features from the video stream and a residual architecture (He et al., 2016) on top of it for predicting the word spoken. The architecture has more than 25 million parameters, occupies 130 MB of disk space and involves 290 million FLOPs for inference. Memory and computation of this order is prohibitively expensive for mobile devices. For instance, the Apple store places a hard limit of 150 MBs on a fully functional app that should include all its components. Furthermore, according to empirical observations made on iOS (StackOverflow, 2019), an app taking more than 50% of the total RAM available at runtime, often crashes.

In addition, performing inference using such models require significant amounts of energy due to memory access and floating point arithmetic (Horowitz, 2014). Table 1 shows energy consumption per operation on an Intel 45nm based system; accessing DRAM consumes \approx 2500 times

* Equal contribution

more energy than floating point addition and therefore dominates energy expenditure. Memory access demands depend on the number of parameters and the intermediate results generated during a forward pass of the neural network, both of which are quite high in all VSR models (Table 2). This means performing inference on VSR model consumes a substantial amount of energy. Therefore, battery drain is a significant issue with such models. Thus, lipreading models, in general, have prohibitively large memory and energy requirements while also making their response-times unacceptable for real-time applications. In this paper, we try to optimize on all four fronts, *i.e.*, memory, time, size and energy while keeping the performance stable. We achieve this using depthwise separable 3D convolution, which we introduce, for the first time, in video classification domain.

Thus, the main contributions we make in this paper are:

- We **generalize 3D convolutions** by using depthwise-separable convolutions and show the applicability of this technique for *the first time* in the video classification domain. This technique helps us to reduce the parameter count and computational complexity vis-a-vis standard convolution (Section 3). This, in turn helps us to achieve better runtime and memory while keeping the accuracy competent.
- We try to provide a new, atomic deep learning construct containing all the optimizations we make, to deep learning practitioners. They can also use this to optimize their models. We call this construct a **LipRes block**. This block also additionally serves as a memory-performance trade-off handle. In the paper, it is modeled as a design hyperparameter, α which allows practitioners to trade off accuracy and model size depending on the use case and constraints. It should be noted that the techniques used in MobiVSR are independent from and complement model compression techniques (Polino et al., 2018; Rastegari et al., 2016; Yu et al., 2017; Han et al., 2015).
- We present the MobiVSR architecture, which for the first time, addresses the problem of deploying visual speech recognition models on **resource constrained devices** (Section 3).
- We show that MobiVSR achieves accuracy of 73% on lipreading in the wild task, in spite of having $6\times$ **fewer parameters** and $20\times$ **smaller model size than the state-of-the-art model**. Us-

ing additional parameter quantization techniques, MobiVSR’s size can be reduced to **6MB** (Appendix Section A.1).

- MobiVSR has been made keeping the following perspectives in mind: first, deployment on mobile platforms and two, general optimization of video recognition architectures. Thus, we perform **energy and environmental cost modelling and comparison** for MobiVSR and all other models (Section 5.1). Comparisons reveal that MobiVSR has *2.9 times lesser* energy impact than other conventional models.

2 Related Work

Research on lip reading spans across centuries (Bulwer, 1648). Several psychological studies have demonstrated that lower level visual information helps in hearing (Demorest and Bernstein, 1991; Dodd and Campbell, 1987). Experiments and research studies have shown that people with (Bernstein et al., 1998; Marschark et al., 1998), and without (Summerfield, 1992), hearing impairment use visual cues for augmenting their understanding of what a speaker is trying to say. As noted by (Chen and Rao, 1998), skilled lip readers look at the configuration and movement of tongue, lips and teeth.

In computational approaches, lip reading is considered as a classification task where the input is a silent video of a speaker utterance and the output is to predict that utterance. Mostly, words or phrases are identified and selected from a limited lexicon, for example just digits (Chen and Rao, 1998; Pachoud et al., 2008; Sui et al., 2015). Early approaches use feature engineering and trains classification models using them (Ngiam et al., 2011; Noda et al., 2015). (Cornu and Milner, 2015), use hand-engineered features to reconstruct audio from video, using a deep-learning network. This method then was modified by (Ephrat et al., 2017) who use a CNN over the entire face of the speaker. Several end-to-end deep learning models have also been developed which rely on a combination of CNN and RNN (Assael et al., 2016; Wand et al., 2016).

Until recently datasets for lipreading were limited by having training sets capturing only a single view of the speakers, and having words from a restricted vocabulary. Recently datasets have become available that contain multiple views (Petridis et al., 2017; Kumar et al., 2018b,a).

Operation	Bit width	Energy (pJ)	Relative Energy consumed per bit
float add	32	0.9	1
float multiply	32	3.7	4.11
DRAM access	64	1300-2600	722.22 - 1444.44

Table 1: Energy expenditure for different operations in 45nm technology (Horowitz, 2014)

(Chung and Zisserman, 2016a) developed a large scale dataset for lip reading with hundreds of distinct words, thousands of instances for each word, and over a thousand speakers. We use this dataset for evaluating MobiVSR (Section 4.1).

Very little work on VSR has focused on developing efficient architectures; however, there is work on this task in image classification and in ASR. The problem of efficient architecture development for image classification was introduced in (Iandola et al., 2016); SqueezeNet achieves accuracy on par with AlexNet (Krizhevsky et al., 2012) but uses far fewer parameters, by using convolutional blocks having 3×3 convolutions followed by 1×1 instead of the large 5×5 kernel used in AlexNet. MobileNet (Howard et al., 2017) uses depthwise-separable convolution (Sifre and Mallat, 2014; Szegedy et al., 2015), for parameter reduction. The MobileNet-V2 architecture (Sandler et al., 2018) improves MobileNet by adding residual connections within the MobileNet depthwise-separable modules. This idea was a major influence in the design of MobiVSR (Section 3).

In the domain of Automatic Speech Recognition (ASR) from audio, a major contribution was PocketSphinx (Huggins-Daines et al., 2006), a large vocabulary, speaker-independent continuous speech recognition engine suitable for handheld devices. More recently, different architectures of compressed RNNs have been proposed for ASR (Prabhavalkar et al., 2016; Mori et al., 2018; Zhang et al., 2018a). (Park et al., 2018) constructs an acoustic model by combining simple recurrent units (SRUs) and depth-wise 1-dimensional convolution layers for multi time step parallelization; this results in reductions in DRAM access and increase in processing speed, allowing real-time on-device ASR on mobile and embedded devices.

Another approach in developing efficient deep learning methods is to redesign computationally expensive layers. For example, Wu et al. (2018) replace standard convolution with a ‘Shift’ layer

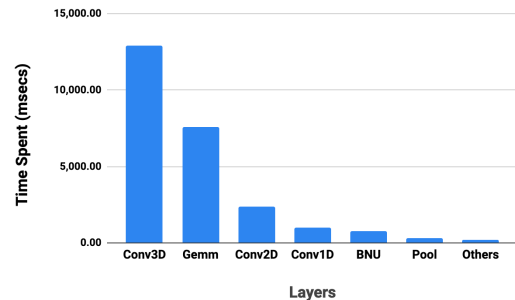


Figure 1: Time spent per layer of the lip reading architecture proposed in (Stafylakis and Tzimiropoulos, 2017), profiled using cProfile.

that consumes zero flops during inference. Zhang et al. (2018b) and Ma et al. (2018) achieve efficiency using a channel shuffle operation. A complementary solution for making deep neural networks suitable for embedded devices is to compress the model post training. This method doesn’t require significant changes in architectural design. Notable examples of this approach include hashing (Chen et al., 2015), quantization (Polino et al., 2018; Wu et al., 2016) and factorization (Lebedev et al., 2014).

3 MobiVSR: End-to-end Lip Reading with Fewer Parameters

This section describes the architecture of MobiVSR along with the explanations behind its design choices.

3.1 The Problem

A brief overview of lipreading models is given in the Table 2. As shown in the table, the size of SOTA model is 130 MBs with a in-memory size of 56.3 MBs. It takes 290 billion FLOPs. With these parameters, it produces a top-3 accuracy of 99.8%. LRW baseline presented in the paper (Chung and Zisserman, 2016b) is also given. However, as mentioned in Section 1, the specifications of both the models are expensive from deployment perspectives, more so for mobile envi-

Model	Size (in MB)	Parameter count (in millions)	Memory access (in thousands)	FLOPs (in billions)	Top-1 accuracy	Top-3 accuracy
LSTM + ResNet (SOTA)	130.0	25.1	56.3	290	83	99.8
LRW Baseline	43.2	8.7	44.0	95.7	61.0	78.0
MobiVSR-1	17.8	4.5	35.3	11.0	72.2	88.0
MobiVSR-2	20.8	5.2	37.3	20.1	73.0	89.0
MobiVSR-3	23.6	5.9	38.9	29.5	73.4	90.2
MobiVSR-4	26.5	6.6	40.4	40.1	74.0	91.0
MobiVSR-10	43.9	10.8	51.5	92.4	77.1	96.1
MobiVSR-11	46.8	11.5	53.3	99.8	77.5	97.3

Table 2: Comparison of accuracy, computational complexity, and memory footprint of MobiVSR (with different α), with the LRW Baseline and the state-of-the-art model. **Note:** MobiVSR-1 denotes the model with $\alpha = 1$

ronments. Thus, after observing these and several other language recognition architectures (Kumar et al., 2018b,a; Petridis and Pantic, 2016; Petridis et al., 2017), we identified the following bottlenecks which limit their deployment avenues:

- All of them use 3D convolutions for processing videos and it is the most compute intensive layer during inference. Figure 1 shows the average percent of inference time spent per layer in the state-of-the-art lip reading system (Stafylakis and Tzimiropoulos, 2017). Thus, this operation, in itself, increases their size and parameter count by several folds (as shown in Section 4.2).
- Most of them use some form of RNNs but RNNs due to their non-parallelizable operations increase the inference time and imposes heavy costs of memory (Bradbury et al., 2016).
- Generally, deep learning practitioners have the tendency to increase number of layers in the hope of getting better performance. This, was also a common observation with lipreading models. For example, the SOTA model contains 51 layers. However, parameter count and memory calls are directly correlated with the number of layers and play a major part in making the models non-usable for mobile environments.

3.2 MobiVSR Architectural Design Choices

The problems presented above (Section 3.1) are the common problems faced by all video recognition tasks. Thus, these problems become our motivation for the design choices of producing an efficient video recognition model, namely, MobiVSR.

Challenge 1. Remove or optimize 3D convolutions: 3D convolutions is a front-end technique in video processing tasks since it can combine information across both time and space (Stafylakis

and Tzimiropoulos, 2017). We observed, doing away with it deteriorates model accuracy. Therefore, optimizing 3D convolution becomes highly important. Inspired by (Howard et al., 2017), where they converted 2D convolution into a sum of depthwise-separable and pointwise convolutions, we generalize 3D convolutions and use this to optimize the front end of the network in our architecture.

Taking a cue from (Ye et al., 2018) and (Howard et al., 2017), we optimize 3D and 2D convolutions with the perspective of making video recognition tasks more efficient. We do it by replacing naive convolutions with depthwise-separable convolutions. By doing this, we get a basic organized deep learning unit, which we call LipRes block. We show its applicability in a language recognition problems using videos (Table 2).

While using depthwise-separable convolutions in 3D, as the first step in any depthwise layer, an important factor to consider was the dimensions of pointwise convolution used. If we represent dimensions as $time \times height \times width$, then the issue is whether to use pointwise convolution of dimension $1 \times 1 \times 1$ (fully pointwise kernel) or $T \times 1 \times 1$ (partial pointwise kernel). The former has the advantage of reducing parameter count more than the latter. While designing the architecture of MobiVSR we found that the latter yields significantly better accuracy as compared to the fully pointwise kernel. We believe this is because in the partial pointwise convolution kernel, the time modality remains intact which is not the case in the fully pointwise kernel. Using $1 \times 1 \times 1$ kernel extracts information independently from each time frame rather than considering multiple frames.

Challenge 2. Avoid RNNs : Recent research in-

dicates that temporal convolutions can be used in place of RNNs without significant loss of accuracy (Bai et al., 2018). Temporal convolutions offer several advantages. They increase parallelism since convolution can process multiple time-steps at once. They also have flexible receptive fields (Mac et al., 2018), and can control model memory usage. Therefore we use 1-D temporal convolution in place of a RNN for modeling temporal features.

Challenge 3. Reduce Parameter Count in Convolution Filters : First, since the kernel parameter count increases quadratically with the kernel size, we had to use small convolution filter sizes of 3×3 in MobiVSR. Due to this constraint, we gained a bonus boost thanks to the modern deep learning frameworks which use several algorithms that optimize the number of operations required for a convolution operation (Chellapilla et al., 2006) with a small filter size (Mathieu et al., 2013; Vasylache et al., 2014; Chetlur et al., 2014; Lavin and Gray, 2016). Second, we use the depthwise-separable convolutions (Howard et al., 2017), for reducing the time and computational complexity of the model.

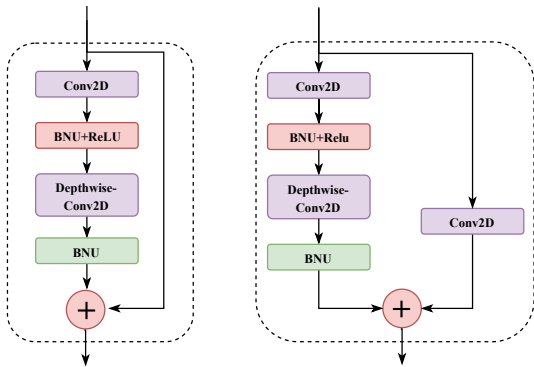


Figure 2: LipRes Blocks: (1) The first LipRes block is for keeping the size of the input constant. It has been used in the first subgraph in MobiVSR. (2) The second LipRes block is for halving the size of the input. It is used in the second, third and the fourth subgraphs in MobiVSR. Thus, increasing alpha by 1, increases the first LipRes block by one and the second LipRes block by 3.

Use Residual Connections : Since increasing the depth of a deep network to increase accuracy adds additional computational complexity and more memory calls, we use residual connections (ResNet blocks) as suggested in (He et al., 2016). These connections are used extensively inside the LipRes block as shown in Fig. 2.

LipRes has a residual structure similar to the ResNet blocks. Each block consists of depthwise-separable convolutions and ReLU (Nair and Hinton, 2010) non linearity, and a parallel skip connection. The use of depthwise separable convolutions and residual connections helps to reduce the parameter count and cut memory calls. The skip connection also has a convolution with stride two whenever the output is supposed to be spatially down-sampled.

Additionally, we use batch normalization (Ioffe and Szegedy, 2015) for regularization. However, contrary to the common paradigm of using batch normalization after every convolution kernel, we use batch normalization scantily as the smaller size of the network has a regularizing effect during training.

Challenge 4. Introduction of LipRes block and varying α : We incorporate solutions to the challenges 1, 2 and 3 in the LipRes block. Through experimentation, we observed that increasing the number of LipRes blocks increased the accuracy but at a cost of making the model heavier and more energy intensive. Thus, we realized that number of LipRes blocks could be leveraged to get a balance between the accuracy and the model size. In the experiments, we show the use of LipRes blocks and also vary its number in order to demonstrate it as a performance-size trade-off handle. For the latter part, we represent the number of blocks by a hyperparameter α which is varied.

3.3 MobiVSR Architecture

The MobiVSR architecture is shown in Figure 3. The MobiVSR model essentially maps visemes (basic units of visual speech) to textual units (*i.e.*, characters/words). Thus, with this in mind, it can be divided into 3 broad parts: (1) a frontend three dimensional convolution part whose function is to extract low level features from visemes; (2) a middle stack of variable sized residual subgraphs whose function is to use those low level features to infer high level features; and (3) a backend consisting of temporal convolutions which essentially functions as a language model of a classical automatic speech recognition system (ASR) by integrating the high-level features to get text out of visemes. Finally, there are two fully connected neural network layers that outputs class probabilities, thus converting abstract grapheme predictions to their probabilities.

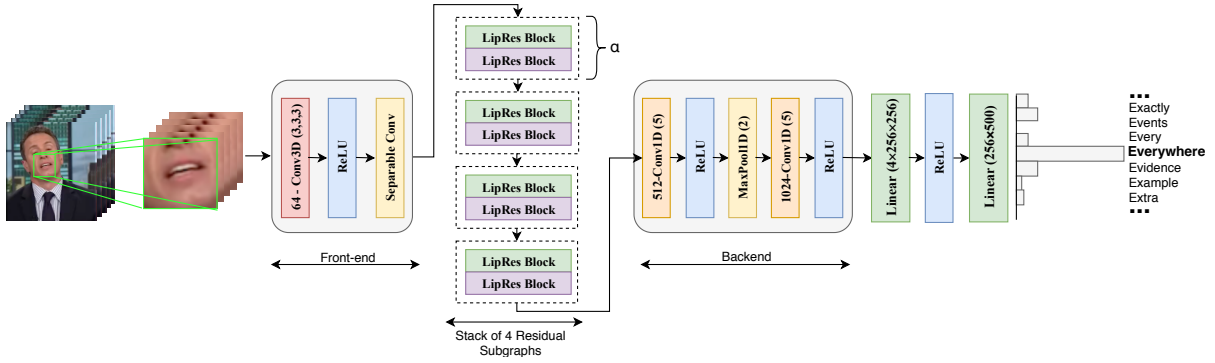


Figure 3: MobiVSR architecture

The front-end part of MobiVSR consists of two 3D depthwise separable convolution layers. We use two depthwise separable layers with kernel size $3 \times 3 \times 3$. Each of these layers downsize the input along spatial dimension by two; we implement this layer by using $3 \times 3 \times 3$ group convolution, with the number of groups being equal to the number of input channels followed by a point-wise spatial convolution kernel of $3 \times 1 \times 1$.

The middle stack of MobiVSR is subdivided into four subgraphs. Each subgraph has α LipRes blocks. Here α is a hyperparameter which one can vary to change the depth of the model. The results pertaining to these are shown in the Table 2, where increasing α increases accuracy but at the cost of using more parameters and vice-versa. Thus, the handle of α makes MobiVSR architecture flexible enough for different applications and environments.

The backend of the model is used to integrate the features across time and provide the word probabilities. Thus, it uses two temporal convolution layers with a Maxpool downsampling sandwiched in between. For performance reasons as outlined above we do not use RNN layers, in contrast to (Stafylakis and Tzimiropoulos, 2017). Finally MobiVSR uses fully connected layers with softmax activation to generate class probabilities for the 500 words in the LRW dataset.

4 Experimental Setup and Results

4.1 Data

We base our experiments on the large publicly available speaker-independent Lip Reading in the Wild (LRW) database (Chung and Zisserman, 2016b). The LRW database contains 1000 utterances each for a collection of 500 different words in the training set. For testing and validation, the

dataset has 50 video clips per class. Each video is challenging because of the high variance of head pose and illumination; therefore, in addition to being one of the few VSR data sets of size, LRW is a good proxy for mobile lip reading data. The video clips are of 29 frames (1.16 seconds) in length, and the speaker mouth region of interest (ROI) is placed at the center of each frame.

A set of 29 consecutive frames (256×256 pixels) is sampled from each video of the LRW Dataset. We then extract the mouth ROI from these RGB frames. As the LRW Dataset is face centered, we achieve this step by cropping a 96×96 pixel window image segment from the center of each frame. Finally, the cropped frame segments are converted to gray scale and stored as numpy matrices (van der Walt et al., 2011). This numpy matrix is then fed to all networks as input.

4.2 Experiments

We train MobiVSR on a NVIDIA Titan X GPU for 50 epochs using six different settings for α (1, 2, 3, 4, 10 and 11). The results are summarized in Table 2. We compare MobiVSR with other word-level lip reading models on saved model size, number of parameters, memory required during inference and number of floating point operations (FLOPs). To ensure consistency in comparing model sizes, we converted each model to ONNX format¹. We calculate inference speeds on an Intel i3 processor and average over 5000 runs. The calculations of memory access and number of floating point operations in different layers are described in Appendix and summarized in Table 3. We ignore the effects of applying non-linearities, batch-normalization and bias terms in these calculations as they do not make significant contributions in

¹<https://onnx.ai>

comparison to matrix multiplications and convolutions. Interested readers can check the appendix for an example and further details regarding the derivation of the expressions as given in Table 3. Energy consumption of various models given in Table 4 has been estimated by multiplying the energy values of various multiplication, addition and memory access provided in Table 1 with their corresponding numbers in Table 3. Furthermore to obtain CO_2 emission estimates, we multiplied the energy consumption values with the average CO_2 emission per kWh of energy as suggested in (Carbonfund.org, 2019).

5 Analysis of Architecture and Results

In this section, we explain the contributions made towards various architectural decisions in results. We also present qualitative evaluation of the results for visual recognition of language.

5.1 Quantitative Formulation

From the Table 2, it can be inferred that MobiVSR-1 achieves 72.2% accuracy on LRW dataset and reaches to an *uncompressed size* of 17.8 MB. As expected, the accuracy increases by increasing the number of LipRes blocks (Section 3). However, several interesting trends can be inferred from the results. One such is the accuracy to size ratio comparison. MobiVSR-1 has an accuracy to size ratio of 4.06 while the SOTA’s value is 0.64. Thus, MobiVSR gives much higher accuracy per megabyte space as compared to any other model. Further, in case of MobiVSR the slope of increase of accuracy vs model size is almost 3 MBs per 100 basis point increase in performance (Figure 4). The statistics of parameter count, memory access and FLOPs also follow the same trends. The values are (SOTA/MobiVSR-1) - FLOPs (0.29/6.56), memory access (1.47/2.04) and parameter count (3.31/16.04). Most of these values show improvements of the order of 10x.

5.2 Qualitative Formulation

While it is quintessential for the model to focus on parameters like memory access, size, parameter count, it is also essential for us to analyse the strengths and weaknesses of the model. Hence we analysed the performance of the model by looking at some specific cases.

While the percentage of true positive predicted by the model is high, there are a few interesting

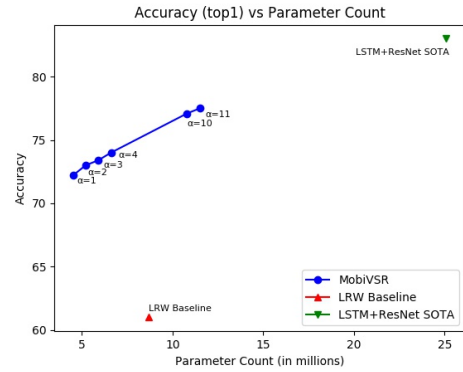


Figure 4: Accuracy vs Parameter Count plot for various values of α

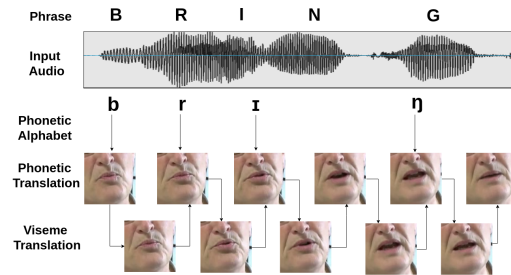


Figure 5: Visemic-phonemic correspondence for the word “Bring”

failure cases as well. We observed that certain samples were not in the dataset, in the dataset samples and human evaluation experiments, some words were being confused with other words. We found out that these are those words which have some common visemes with other words. For example, take the case of these two words: ‘bring’ and ‘being’ as presented in Figures 5 and 6. ‘Bring’ has the following visemes: $\{E, A, V4, H\}$ and ‘Being’ has the following: $\{E, V4, V4, H\}$ (Neti et al., 2000). As can be seen in the figures, three out of four visemes are common in both of them. The fourth ones which are different are spoken from within the mouth, hence are difficult to capture using a camera. The model confuses between them 80% of the time. We observed similar behaviour with these pairs as well: $\{Billions, Millions\}$, $\{Having, Heavy\}$, $\{General, Several\}$, etc.

Several such cases are documented in the Table 5. The last two rows in the table contain those words which are not confused with any other words. As can be observed (by speaking those words) that those words do not contain many phonemes or even visemes in common. This should be the reason why they aren’t confused.

Layer	Memory Access	Floating point operations (FLOPs)
Conv2D	$K^2 C_i C_o + V_i \cdot (K^2 C_o) + V_o$	$2(K^2 C_i) \cdot V_o$
Conv3D	$K^2 T C_i C_o + V_i \cdot (K^2 C_o) \cdot T + V_o$	$2(K^2 T C_i) \cdot V_o$
Depthwise Separable Conv2D	$C_i \cdot (K^2 + C_o) + V_i \cdot (K^2 + C_o) + V_o$	$2C_i \cdot (\frac{K^2}{C_o} + 1) \cdot V_o$
Depthwise Separable Conv3D	$C_i \cdot (K^2 + C_o) \cdot T + V_i \cdot (K^2 + C_o) \cdot T + V_o$	$2C_i \cdot (\frac{K^2}{C_o} + 1) \cdot T \cdot V_o$
Fully Connected	$IQ + V_i + V_o$	$2IQ$

Table 3: Number of memory access and FLOPs associated with different layers. V_i and V_o are the input and output volume respectively. C_i and C_o are the input and output channel dimensions. $K \times K$ is the 2D convolution kernel while $K \times K \times T$ is the 3D convolution kernel

Model	Energy Consumed per Inference (milli Joules)	CO_2 emitted per Inference (mg)
MobiVSR-1	25.37	3.21
MobiVSR-2	46.30	5.85
MobiVSR-3	67.92	8.59
MobiVSR-4	92.31	11.67
MobiVSR-10	212.62	26.89
MobiVSR-11	229.64	29.01
LSTM + ResNet	667.11	84.38
LRW Baseline	229.39	29.01

Table 4: Comparison of models on the basis of energy consumed and CO_2 emission per inference.

Table 5: Some sample words and what are they getting confused against. The first two rows contain maximally confusing words, the next two contain average cases and the last two the least confused words.

Word	Confusion	Word	Confusion
Benefits	Benefit	Spent	Spend
Price	Press	Living	Giving
Words	Workers	These	Years
Action	Actually	Community	Abuse
About	Afternoon	About	Weapons
About	Temperatures	About	Westminster

Using these error cases, we discover that model, when it fails, fails due to the signals which cannot be captured using a camera only. For example, the sound of ‘ba’ in billions and ‘ma’ in millions belong to the same viseme class but map to different phonemes. Thus, a camera alone cannot capture and differentiate between these two, however, when coupled with an audio-recording device, signals from both of them combined can potentially help to discriminate amongst them ².

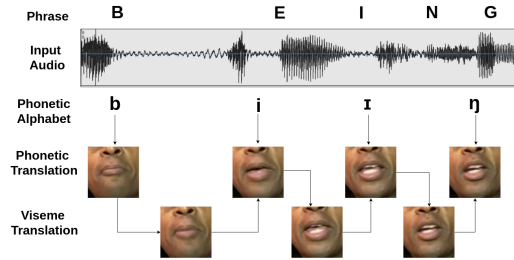


Figure 6: Visemic-phonemic correspondence for the word ‘Being’

6 Conclusion and Future Work

In this paper we introduced MobiVSR, a deep neural network model designed to perform word level visual speech recognition in resource constrained devices. We showed how MobiVSR uses $6 \times$ less parameters than the state-of-the-art model and can be compressed to 6MB after quantization. Moreover it can be modified using a tuneable hyperparameter to balance accuracy and efficiency for different use cases. As mentioned earlier, mobile-centric lip reading systems have enormous utility in the society. We hope that this paper inspires other researchers to create similar and even

²Since LRW is a dataset which is quite close to real environment, we perform some experiments on some people who were not present in the dataset. Images of one such sample is given in the appendix.

more efficient models considering the social impact such applications can have.

References

- Yannis M Assael, Brendan Shillingford, Shimon Whiteson, and Nando De Freitas. 2016. Lipnet: End-to-end sentence-level lipreading. *arXiv preprint arXiv:1611.01599*.
- Shaojie Bai, J Zico Kolter, and Vladlen Koltun. 2018. An empirical evaluation of generic convolutional and recurrent networks for sequence modeling. *arXiv preprint arXiv:1803.01271*.
- Lynne E Bernstein, Marilyn E Demorest, and Paula E Tucker. 1998. What makes a good speechreader? first you have to find one. *Hearing by eye II: Advances in the psychology of speechreading and auditory-visual speech*, pages 211–227.
- James Bradbury, Stephen Merity, Caiming Xiong, and Richard Socher. 2016. Quasi-recurrent neural networks. *arXiv preprint arXiv:1611.01576*.
- John Bulwer. 1648. *Philocopus, or the deaf and dumbe mans friend*, london: Humphrey and moseley.
- Carbonfund.org. 2019. [Co2 emission calculation](#).
- Kumar Chellapilla, Sidd Puri, and Patrice Simard. 2006. High performance convolutional neural networks for document processing. In *Tenth International Workshop on Frontiers in Handwriting Recognition*. Suvisoft.
- Tsuhan Chen and Ram R Rao. 1998. Audio-visual integration in multimodal communication. *Proceedings of the IEEE*, 86(5):837–852.
- Wenlin Chen, James Wilson, Stephen Tyree, Kilian Weinberger, and Yixin Chen. 2015. Compressing neural networks with the hashing trick. In *International Conference on Machine Learning*, pages 2285–2294.
- Sharan Chetlur, Cliff Woolley, Philippe Vandermersch, Jonathan Cohen, John Tran, Bryan Catanzaro, and Evan Shelhamer. 2014. cudnn: Efficient primitives for deep learning. *arXiv preprint arXiv:1410.0759*.
- Joon Son Chung, Andrew Senior, Oriol Vinyals, and Andrew Senior. 2017. Lip reading sentences in the wild. In *2017 IEEE Conference on Computer Vision and Pattern Recognition (CVPR)*, pages 3444–3453. IEEE.
- Joon Son Chung and Andrew Senior. 2016a. Lip reading in the wild. In *Asian Conference on Computer Vision*, pages 87–103. Springer.
- Joon Son Chung and Andrew Senior. 2016b. Lip reading in the wild. In *Asian Conference on Computer Vision*, pages 87–103. Springer.
- Thomas Le Cornu and Ben Milner. 2015. Reconstructing intelligible audio speech from visual speech features. In *Sixteenth Annual Conference of the International Speech Communication Association*.
- Marilyn E Demorest and Lynne E Bernstein. 1991. Computational explorations of speechreading. *Journal of the Academy of Rehabilitative Audiology*.
- Barbara Ed Dodd and Ruth Ed Campbell. 1987. *Hearing by eye: The psychology of lip-reading*. Lawrence Erlbaum Associates, Inc.
- Ariel Ephrat, Tavi Halperin, and Shmuel Peleg. 2017. Improved speech reconstruction from silent video. In *Proceedings of the IEEE International Conference on Computer Vision*, pages 455–462.
- Song Han, Huizi Mao, and William J Dally. 2015. Deep compression: Compressing deep neural networks with pruning, trained quantization and Huffman coding. *arXiv preprint arXiv:1510.00149*.
- Kaiming He, Xiangyu Zhang, Shaoqing Ren, and Jian Sun. 2016. Deep residual learning for image recognition. In *Proceedings of the IEEE conference on computer vision and pattern recognition*, pages 770–778.
- Mark Horowitz. 2014. 1.1 computing’s energy problem (and what we can do about it). In *Solid-State Circuits Conference Digest of Technical Papers (ISSCC), 2014 IEEE International*, pages 10–14. IEEE.
- Andrew G Howard, Menglong Zhu, Bo Chen, Dmitry Kalenichenko, Weijun Wang, Tobias Weyand, Marco Andreetto, and Hartwig Adam. 2017. Mobilenets: Efficient convolutional neural networks for mobile vision applications. *arXiv preprint arXiv:1704.04861*.
- David Huggins-Daines, Mohit Kumar, Arthur Chan, Alan W Black, Mosur Ravishankar, and Alexander I Rudnicky. 2006. Pocketsphinx: A free, real-time continuous speech recognition system for hand-held devices. In *2006 IEEE International Conference on Acoustics Speech and Signal Processing Proceedings*, volume 1, pages I–I. IEEE.
- Forrest N Iandola, Song Han, Matthew W Moskewicz, Khalid Ashraf, William J Dally, and Kurt Keutzer. 2016. Squeezenet: Alexnet-level accuracy with 50x fewer parameters and 0.5 mb model size. *arXiv preprint arXiv:1602.07360*.
- Sergey Ioffe and Christian Szegedy. 2015. Batch normalization: Accelerating deep network training by reducing internal covariate shift. *arXiv preprint arXiv:1502.03167*.
- Alex Krizhevsky, Ilya Sutskever, and Geoffrey E Hinton. 2012. Imagenet classification with deep convolutional neural networks. In *Advances in neural information processing systems*, pages 1097–1105.

- Yaman Kumar, Mayank Aggarwal, Pratham Nawal, Shin'ichi Satoh, Rajiv Ratn Shah, and Roger Zimmermann. 2018a. Harnessing ai for speech reconstruction using multi-view silent video feed. In *2018 ACM Multimedia Conference on Multimedia Conference*, pages 1976–1983. ACM.
- Yaman Kumar, Rohit Jain, Mohd Salik, Rajiv ratn Shah, Roger Zimmermann, and Yifang Yin. 2018b. Mylipper: A personalized system for speech reconstruction using multi-view visual feeds. In *2018 IEEE International Symposium on Multimedia (ISM)*, pages 159–166. IEEE.
- Andrew Lavin and Scott Gray. 2016. Fast algorithms for convolutional neural networks. In *Proceedings of the IEEE Conference on Computer Vision and Pattern Recognition*, pages 4013–4021.
- Vadim Lebedev, Yaroslav Ganin, Maksim Rakhuba, Ivan Oseledets, and Victor Lempitsky. 2014. Speeding-up convolutional neural networks using fine-tuned cp-decomposition. *arXiv preprint arXiv:1412.6553*.
- Ningning Ma, Xiangyu Zhang, Hai-Tao Zheng, and Jian Sun. 2018. Shufflenet v2: Practical guidelines for efficient cnn architecture design. In *Proceedings of the European Conference on Computer Vision (ECCV)*, pages 116–131.
- Khoi-Nguyen C Mac, Dhiraj Joshi, Raymond A Yeh, Jinjun Xiong, Rogerio R Feris, and Minh N Do. 2018. Locally-consistent deformable convolution networks for fine-grained action detection. *arXiv preprint arXiv:1811.08815*.
- Marc Marschark, Dominique LePoutre, and Linda Bement. 1998. *Mouth movement and signed communication*. Hove, United Kingdom: Psychology Press Ltd. Publishers.
- Michael Mathieu, Mikael Henaff, and Yann LeCun. 2013. Fast training of convolutional networks through ffts. *arXiv preprint arXiv:1312.5851*.
- Takuma Mori, Andros Tjandra, Sakriani Sakti, and Satoshi Nakamura. 2018. Compressing end-to-end asr networks by tensor-train decomposition. *Proc. Interspeech 2018*, pages 806–810.
- Stephen P Morse, William B Pohlman, and Bruce W Ravenel. 1978. The intel 8086 microprocessor: a 16-bit evolution of the 8080. *Computer*, (6):18–27.
- Vinod Nair and Geoffrey E Hinton. 2010. Rectified linear units improve restricted boltzmann machines. In *Proceedings of the 27th international conference on machine learning (ICML-10)*, pages 807–814.
- Chalapathy Neti, Gerasimos Potamianos, Juergen Luetin, Iain Matthews, Herve Glotin, Dimitra Vergyri, June Sison, Azad Mashari, and Jie Zhou. 2000. Audio-visual speech recognition. In *Final workshop*, pages 40–41.
- Jiquan Ngiam, Aditya Khosla, Mingyu Kim, Juhan Nam, Honglak Lee, and Andrew Y Ng. 2011. Multimodal deep learning. In *Proceedings of the 28th international conference on machine learning (ICML-11)*, pages 689–696.
- Kuniaki Noda, Yuki Yamaguchi, Kazuhiro Nakadai, Hiroshi G Okuno, and Tetsuya Ogata. 2015. Audio-visual speech recognition using deep learning. *Applied Intelligence*, 42(4):722–737.
- Samuel Pachoud, Shaogang Gong, and Andrea Cavallaro. 2008. Macro-cuboid based probabilistic matching for lip-reading digits. In *2008 IEEE Conference on Computer Vision and Pattern Recognition*, pages 1–8. IEEE.
- Jinhwan Park, Yoonho Boo, Iksoo Choi, Sungho Shin, and Wonyong Sung. 2018. Fully neural network based speech recognition on mobile and embedded devices. In *Advances in Neural Information Processing Systems*, pages 10642–10653.
- Stavros Petridis and Maja Pantic. 2016. Deep complementary bottleneck features for visual speech recognition. In *2016 IEEE International Conference on Acoustics, Speech and Signal Processing (ICASSP)*, pages 2304–2308. IEEE.
- Stavros Petridis, Yujiang Wang, Zuwei Li, and Maja Pantic. 2017. End-to-end multi-view lipreading. *arXiv preprint arXiv:1709.00443*.
- Antonio Polino, Razvan Pascanu, and Dan Alistarh. 2018. Model compression via distillation and quantization. *arXiv preprint arXiv:1802.05668*.
- Rohit Prabhavalkar, Ouais Alsharif, Antoine Bruguier, and Lan McGraw. 2016. On the compression of recurrent neural networks with an application to lvcxr acoustic modeling for embedded speech recognition. In *2016 IEEE International Conference on Acoustics, Speech and Signal Processing (ICASSP)*, pages 5970–5974. IEEE.
- Mohammad Rastegari, Vicente Ordonez, Joseph Redmon, and Ali Farhadi. 2016. Xnor-net: Imagenet classification using binary convolutional neural networks. In *European Conference on Computer Vision*, pages 525–542. Springer.
- Mark Sandler, Andrew Howard, Menglong Zhu, Andrey Zhmoginov, and Liang-Chieh Chen. 2018. Mobilenetv2: Inverted residuals and linear bottlenecks. *arXiv preprint arXiv:1801.04381*.
- Laurent Sifre and Stéphane Mallat. 2014. *Rigid-motion scattering for image classification*. Ph.D. thesis, Citeseer.
- StackOverflow. 2019. [ios - experiments for maximum runtime memory accesses allowed](#).
- Themos Stafylakis and Georgios Tzimiropoulos. 2017. Combining residual networks with lstms for lipreading. *arXiv preprint arXiv:1703.04105*.

- Chao Sui, Mohammed Bennamoun, and Roberto Togneri. 2015. Listening with your eyes: Towards a practical visual speech recognition system using deep boltzmann machines. In *Proceedings of the IEEE International Conference on Computer Vision*, pages 154–162.
- Quentin Summerfield. 1992. Lipreading and audio-visual speech perception. *Philosophical Transactions of the Royal Society of London. Series B: Biological Sciences*, 335(1273):71–78.
- Christian Szegedy, Wei Liu, Yangqing Jia, Pierre Sermanet, Scott Reed, Dragomir Anguelov, Dumitru Erhan, Vincent Vanhoucke, and Andrew Rabinovich. 2015. Going deeper with convolutions. In *Proceedings of the IEEE conference on computer vision and pattern recognition*, pages 1–9.
- Nicolas Vasilache, Jeff Johnson, Michael Mathieu, Soumith Chintala, Serkan Piantino, and Yann LeCun. 2014. Fast convolutional nets with fbfft: A gpu performance evaluation. *arXiv preprint arXiv:1412.7580*.
- Stfan van der Walt, S Chris Colbert, and Gael Varoquaux. 2011. [The numpy array: A structure for efficient numerical computation](#). *Computing in Science & Engineering*, 13:22 – 30.
- Michael Wand, Jan Koutník, and Jürgen Schmidhuber. 2016. Lipreading with long short-term memory. In *2016 IEEE International Conference on Acoustics, Speech and Signal Processing (ICASSP)*, pages 6115–6119. IEEE.
- Bichen Wu, Alvin Wan, Xiangyu Yue, Peter Jin, Sicheng Zhao, Noah Golmant, Amir Gholaminejad, Joseph Gonzalez, and Kurt Keutzer. 2018. Shift: A zero flop, zero parameter alternative to spatial convolutions. In *Proceedings of the IEEE Conference on Computer Vision and Pattern Recognition*, pages 9127–9135.
- Jiaxiang Wu, Cong Leng, Yuhang Wang, Qinghao Hu, and Jian Cheng. 2016. Quantized convolutional neural networks for mobile devices. In *Proceedings of the IEEE Conference on Computer Vision and Pattern Recognition*, pages 4820–4828.
- Rongtian Ye, Fangyu Liu, and Liqiang Zhang. 2018. 3d depthwise convolution: Reducing model parameters in 3d vision tasks. *arXiv preprint arXiv:1808.01556*.
- Xiyu Yu, Tongliang Liu, Xinchao Wang, and Dacheng Tao. 2017. On compressing deep models by low rank and sparse decomposition. In *Proceedings of the IEEE Conference on Computer Vision and Pattern Recognition*, pages 7370–7379.
- Jie Zhang, Xiaolong Wang, Dawei Li, and Yalin Wang. 2018a. Dynamically hierarchy revolution: dirnet for compressing recurrent neural network on mobile devices. *arXiv preprint arXiv:1806.01248*.
- Xiangyu Zhang, Xinyu Zhou, Mengxiao Lin, and Jian Sun. 2018b. Shufflenet: An extremely efficient convolutional neural network for mobile devices. In *The IEEE Conference on Computer Vision and Pattern Recognition (CVPR)*.

A Appendices

A.1 Calculating memory access

In order to estimate memory access we make some simplifying assumptions. First, to get a fair comparison we neglect the effect of computer architecture dependent optimizations. Second, for comparing memory usage by different models, we focus on two aspects that lead to memory consumption: i) memory read operations for model parameters, and ii) the memory read by a layer to read input and write its output. Third, we assume that during the forward pass, model weights are read once and then used as long as required in one pass. Each read and write is counted as one memory access. This is not necessarily true in all cases as some computing environments can read more than one value in a single memory access (Morse et al., 1978). For the sake of simplicity we ignore such architectural characteristics.

Memory access in convolutions - For a 3D-kernel, with T the kernel size along the temporal dimension, the number of parameters is given by $P_{conv3d}=K^2TC_iC_o$. Depthwise separable convolutions can be thought of as a two step process. The first part consists of convolving each channel separately which is then followed by a pointwise convolution across the full channel length of the input. As mentioned in (Howard et al., 2017), the number of parameters in a two dimensional depthwise separable convolution is given by $P_{depth2d}=C_i \cdot (K^2+C_o)$. The first term is the cost of the first step in a depthwise separable kernel and the second term is the cost of applying C_o number of pointwise kernels as part of the second step. By the same logic, generalising the number of parameters to a three dimensional depthwise separable convolution layer, we get:

$$P_{depth3d}=C_i \cdot (K^2+C_o) \cdot (T) \quad (1)$$

To calculate the number of memory reads, consider the following case. If the input has dimensions $I \times I \times C_i$ (where $I \times I$ is the height and width of the input matrix and C_i is the channel length), then for each convolution in two dimensions with a $K \times K$ kernel, each element of the input matrix will be loaded from memory $K \times K$ times. Since there are C_o number of such kernels, each element will be read $K \times K \times C_o$ times. So the number of times input memory read operations will be performed is given by

$$R_{conv2d}=(I^2C_i) \cdot (K^2C_o) \quad (2)$$

Here I^2C_i is the input volume V_i . So we can rewrite Eq. 2 as $R_{conv2d}=V_i \cdot (K^2C_o)$. Similarly for each three dimensional convolution the number of memory read operations is $R_{conv3d}=(I^2L_iC_i) \cdot (K^2C_o) \cdot T$. Putting $V_i=I^2L_iC_i$ where V_i is the input volume to 3D convolution, we get

$$R_{conv3d}=V_i \cdot (K^2C_o) \cdot T \quad (3)$$

In case of two dimensional depthwise separable convolutions, each element of the input matrix is convolved $K \times K \times 1$ in the first step. Since each input channel has a separate spatial kernel in this step, the number of memory reads turn out to be $I \times I \times K \times K \times 1 \times C_i$. The resultant matrix then undergoes pointwise convolution which requires $I \times I \times C_i \times 1 \times 1 \times C_o$ memory reads. Therefore the total number of input read operations in performing a two dimensional depthwise separable convolution is

$$R_{depth2d}=I^2 \times K^2 \times 1 \times C_i + I^2 \times C_i \times 1^2 \times C_o = (I^2C_i) \cdot (K^2+C_o) \quad (4)$$

which can be written as

$$R_{depth2d}=V_i \cdot (K^2+C_o) \quad (5)$$

Extending the argument to three dimensions, the number of input memory read associated with a 3D depthwise convolution layer is

$$R_{depth3d}=(I^2C_iL_i) \cdot (K^2+C_o) \cdot T \quad (6)$$

which is the same as

$$R_{depth3d}=V_i \cdot (K^2+C_o) \cdot T \quad (7)$$

Memory accessed due to memory write operations for storing the output of the convolution is simply equal to the size of the output V_o . Therefore the total memory access M_{acc} in convolution layers can be obtained by adding the respective R_s, P_s and V_o .

Memory access in fully connected layers - A fully connected layer which takes an I element vector and outputs a Q element vector is essentially a $I \times Q$ weight matrix. Therefore the number of parameters in a fully connected layer is equal to the size of this matrix $P_{fc}=IQ$. Since this layer is just a matrix multiplication, the input matrix needs to be read once. Hence the number of input memory read operations is simply equal to the number of elements in the input. Similar to convolution layers, the number of memory write operations in a fully connected layer is equal to the size of the output.

A.2 Calculation of FLOPs

To calculate the number of FLOPs in convolutions and fully connected layers, it is important to note that these operations involve element-wise multiplication (of the kernel elements with a specific region of the input feature map) followed by an addition (accumulation) of all the products obtained. For instance a dot product of two n element vectors has n element-element multiplications and $n-1$ additions. The total number of FLOPs in an n element dot product is $2n-1$. As $n \gg 1$, this could be approximated as $2n$.

FLOPs in Convolutions - In the case of a two dimensional convolution, we can think of the process of convolving over a region as the dot product between the kernel weights and the input region below it. This dot-product has $K \times K \times C_i$ elements. Therefore this operation requires $2 \times K \times K \times C_i$ FLOPs. This process happens for every element of the output feature map of size $H \times H$, repeated for C_o convolution kernels. Therefore the total number of FLOPs is

$$F_{conv2d} = 2K^2 C_i H^2 C_o \quad (8)$$

Here $H^2 C_o$ is simply the output volume V_o . Therefore $F_{conv2d} = 2(K^2 C_i) \cdot V_o$. Similarly in three dimensions this number is $F_{conv3d} = 2H^2 L_o C_i K^2 T C_o$. As $V_o = H^2 L_o C_o$, we can write the above equation as

$$F_{conv3d} = 2(K^2 T C_i) \cdot V_o \quad (9)$$

The first step of a depthwise separable convolution is similar to a normal convolution, except the dot products involve $K \times K \times 1$ elements along each one of the C_i input channels. Similar to simple convolutions, this is done for each $H \times H$ output element. This results in $2 \times K^2 \times C_i \times H \times H$ FLOPs.

The pointwise convolution step involves dot products of C_i done for every $H \times H$ output pixel. As there are C_o of these pointwise kernels the FLOPs required in this step are $2 \times 1^2 \times C_i \times H^2 \times C_o$. Therefore the total number of FLOPs is

$$F_{depth2d} = 2(H^2 C_i) \cdot (K^2 + C_o) \quad (10)$$

Again putting $V_o = H^2 C_o$ we get $F_{depth2d} = 2C_i \cdot (\frac{K^2}{C_o} + 1) \cdot V_o$. By the same logic, the number of FLOPs in a three dimensional depthwise convolution layers is given by $F_{depth3d} = 2(H^2 L_o C_i) \cdot (K^2 + C_o) \cdot T$, which is the same as

$$F_{depth3d} = 2C_i \cdot (\frac{K^2}{C_o} + 1) \cdot T \cdot V_o \quad (11)$$

FLOPs in Fully Connected Layers - Since a fully connected layer is a $I \times Q$ matrix where I is the size of the input vector, the matrix multiply as part of the fully connected layer can be thought of as a dot product between the I element input and column vectors of the matrix which is repeated Q times. Therefore the number of FLOPs in a fully connected layer is $F_{fc} = 2IQ$.

Table 3, summarizes all the equations used for calculating memory accesses and number of FLOPs by different layers in our proposed architecture. As an example a 2D convolution layer with kernel size 3 with 64 as output channel size. Suppose the input is of the shape $100 \times 100 \times 3$. From Table 3 the number of memory access are $(100^2 \cdot 3 \cdot 64) + (100 \cdot 100 \cdot 3) \cdot (100^2 \cdot 64) + (100^2 \cdot 64) \sim 1.94 \times 10^8$. Similarly FLOPs would be $2(100^2 \cdot 3) \cdot (100^2 \cdot 64) \sim 3.8 \times 10^{10}$.